

Use of simultaneous depth and MEG recording may provide complementary information regarding the epileptogenic region

Yosuke Kakisaka^{1,2}, Yuichi Kubota¹, Zhong I. Wang¹, Zhe Piao¹, John C. Mosher¹, Jorge Gonzalez-Martinez³, Kazutaka Jin⁴, Andreas V. Alexopoulos¹, Richard C. Burgess¹

¹ Department of Neurology, The Cleveland Clinic, Cleveland, OH, USA

² Department of Pediatrics, Tohoku University School of Medicine, Sendai, Japan

³ Department of Neurosurgery, The Cleveland Clinic, Cleveland, OH, USA

⁴ Department of Epileptology, Tohoku University School of Medicine, Sendai, Japan

Received December 20, 2011; Accepted May 29, 2012

ABSTRACT – Simultaneous SEEG-MEG recording has the potential to define the epileptic spike source accurately. We present a case of a 55-year-old female with intractable left temporal lobe epilepsy in whom we evaluated the relationship between the amplitude recorded from SEEG electrodes, inserted in the lateral temporal region, and their distance from the MEG-modelled spike. We found a quadratic fall-off relationship between the amplitude and distance. This result supports the concept that the MEG dipoles reflect the “centre” of spike locations and may provide comprehensive information for SEEG which records spike activities directly but is inherently limited in spatial sampling.

Key words: stereotactic electroencephalography, magnetoencephalography, simultaneous recording, volume conduction, quadratic fall-off

Although different in their invasiveness, both stereotactic electroencephalography (SEEG) and magnetoencephalography (MEG) have important and complementary roles in the evaluation of epilepsy surgical candidates. The advantage of SEEG is that it records epileptic activity directly from brain parenchyma itself, but the sparsely and irregularly placed electrodes limit spatial sampling (Talairach *et al.*, 1962;

Spencer, 1981). MEG cannot easily detect deep, low-amplitude signals, but has the advantages of providing extensive spatial sampling and precise non-invasive localisation of epileptic activity (Knowlton *et al.*, 1997). With regards to spike detection, although MEG is sensitive to magnetic fields reflecting intracellular neuronal currents and extracellular currents of the spike itself are detected by SEEG, both

Correspondence:

Yosuke Kakisaka
Epilepsy Center,
Department of Neurology,
The Cleveland Clinic Foundation,
9500 Euclid Avenue,
Cleveland, OH 44195, USA
<kakisuke@mui.biglobe.ne.jp>

reflect the same phenomenon; excitation of neurons (Hari and Lounasmaa, 1989). With the whole-head MEG arrays and multi-contact invasive electrodes available today, simultaneous SEEG-MEG (sSEEG-MEG) combines the advantages of these two modalities, which may “fill in the gaps” left by the individual modalities, as recently reported by Wang *et al.* (2012). Utility of sSEEG-MEG should enhance our ability to construct an effective strategy for epilepsy surgery.

Epileptic sources are localised using MEG by modelling activity as a single equivalent current dipole. In order to optimise the use of sSEEG-MEG, it is important to understand the relationship between MEG and SEEG data; most importantly, the magnitude of spike activity from SEEG electrodes and the MEG spike dipole position. We set out to quantitatively characterise these amplitude relationships in three dimensions by analysing epileptic spikes recorded during sSEEG-MEG, in a patient with intractable focal epilepsy.

Case report and methods

A 55-year-old female patient had previously undergone a left lateral temporal lobe resection for intractable left temporal lobe epilepsy. After the surgery, she had recurring seizures, therefore, further invasive study was considered.

At evaluation, SEEG electrode implantation was chosen. The electrodes consisted of 8-12 cylindrical 2.5 mm-long platinum contacts with 1.1 mm diameter, separated by 5 mm (INTEGRA EPILEPSY™, INTEGRA, NJ, USA). In this study, 10 SEEG electrodes were inserted which allowed us to observe spikes from various regions in the left hemisphere (*figure 1*). Details of the implantation were as follows: B': head of

hippocampus; C': middle temporal gyrus; E': anterior basal temporal; F': posterior basal temporal; O': infracalcarine; P': posterior parietal; U': superior temporal gyrus; V': supracalcarine, W': anterior parietal; and X': supramarginal region (*figure 1A and 1B*). SEEG and MEG were simultaneously recorded in a magnetically-shielded room. This study received approval from the Cleveland Clinic Institutional Review Board (IRB 09-934). SEEG signals were sampled at 1000 Hz and band-pass filtered between 0.5 and 70 Hz. With the patient in the supine position, MEG data were recorded with a whole-head MEG system with 204 planar gradiometers (VectorView; Neuromag, Helsinki, Finland). MEG signals were sampled at 1000 Hz, band-pass filtered between 0.5 and 70 Hz and recorded for 30-minute periods during awake and sleep conditions. We also applied continuous movement compensation algorithm during recording (Medvedovsky *et al.*, 2007). Before MEG analysis, we performed temporally-extended signal space separation algorithm (tSSS) to each MEG data set with a commercial software package, “MaxFilter”, to eliminate magnetic noise, the details of which are described elsewhere (Song *et al.*, 2009). The acquired data were low-pass filtered at 50 Hz. High-pass filtering was used at 6 Hz to extract the spike component from the slower background activity. After 30 minutes of sSEEG-MEG recording, two types of left temporal spikes were captured by SEEG; one from the lateral temporal region ($n=79$) and the other from the basal temporal region ($n=7$). Of the 79 spikes from the lateral temporal group, 51 spikes (65%) were also captured using MEG (SEEG+/MEG+); the remaining 28 spikes (35%) were not observed using MEG (SEEG+/MEG-). No spikes detected only by MEG (SEEG-/MEG+) were observed in the lateral temporal group. The extent of lateral temporal SEEG contacts involved

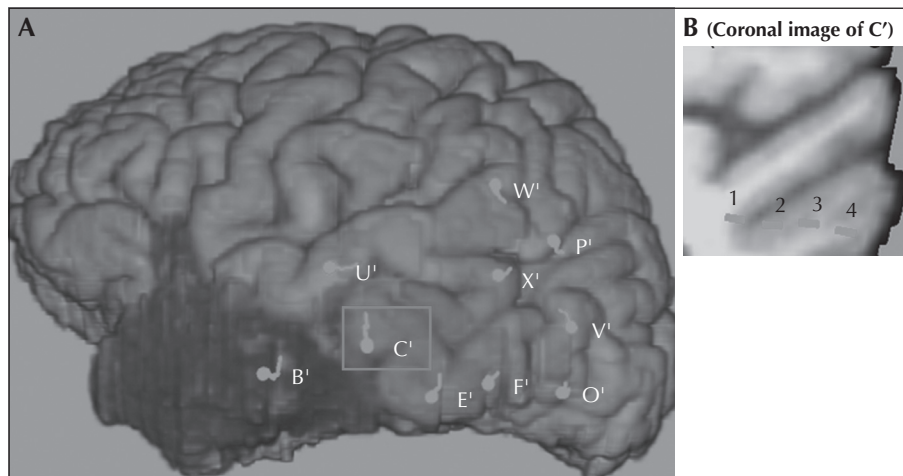


Figure 1. (A) Reconstructed three dimensional brain surface image including the penetration points of all stereotactic EEG (SEEG) electrodes. (B) Coronal view of MRI showing C' contacts inserted in the left lateral temporal region. Cylinders indicate C' SEEG contacts; C'1 is the most mesial contact and C'4 the most lateral.

(C') was variable between groups. In the SEEG+/MEG+ group, three contacts were activated for 26 spikes and four or more contacts were activated for 25 spikes. In the SEEG+/MEG- group, two contacts were activated for 14 spikes and three contacts activated for 14 spikes, and there were no spikes involving four or more contacts. Of seven spikes from the basal temporal region, none were captured using MEG and no spikes detected only by MEG were observed (SEEG+/MEG-; 100%).

To investigate the spatial relationship between the magnitude of the SEEG spike and location of the MEG spike, we selected SEEG+/MEG+ spikes from the lateral temporal region using the following criteria: 1) MEG spike was outstanding and distinguishable from background activity (>2 fold amplitude above background activity), and 2) simultaneously recorded SEEG also showed counterpart activity and the data from all four depth contacts were available. The amplitude of SEEG spike, in which the right mastoid electrode was used as reference, was calculated from the peak to trough measurement as shown in *figure 2* (Matsumoto *et al.*, 2004).

The present study analysed the generator's location of the main MEG spike peak. Single dipole modelling was applied on MEG signals in a spherical head model using vendor source modelling software (Neuromag, Helsinki, Finland). Equivalent current dipoles (ECDs) of spikes with a goodness-of-fit over 90% were regarded as reliable. MRI before SEEG electrode insertion (pre-operative MRI), acquired as three-dimensional volume (1.5 T, MP-RAGE sequence, Siemens, Germany) was used for three dimensional images. High resolution CT after SEEG electrode insertion (postoperative CT) was acquired at 1 mm thickness and coregistered with pre-operative MRI. The coordinates of the SEEG electrodes were then superimposed onto preoperative MRI. In the reconstruction, the shape and orientation of the electrode contacts were emulated as closely as possible to the physical dimension and actual orientation in the brain (*figure 3A and 3B*). Finally, estimated ECDs were superimposed onto the patient's MRI. These details have been described elsewhere (Matsumoto *et al.*, 2004). On this integrated MRI, a built-in tool allowed us, not only to see the spike dipoles superimposed on the patient's MRI, but also to measure the distance from the centre of each SEEG contact to the centre of each MEG spike dipole.

Only eight of the recorded interictal spikes met the selection criteria due to incomplete recording from SEEG electrodes, caused by technical difficulty. For each spike, the amplitude (y axis) versus the distance from the calculated dipole to each SEEG contact (d) was plotted and approximated with a quadratic fall-off curve based on methodology consistent with the literature (Patton and Woodbury, 1965).

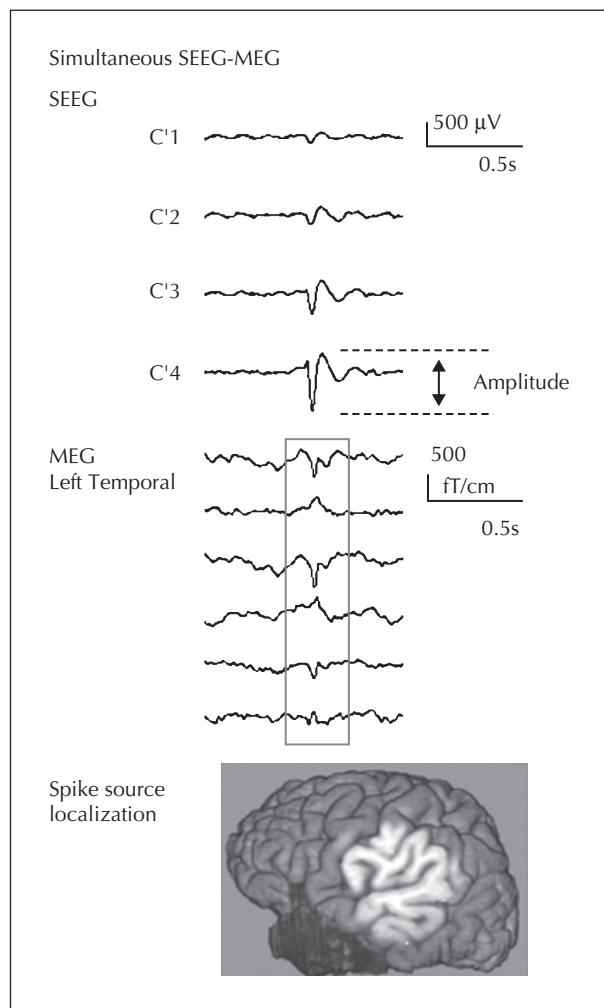


Figure 2. Waveform of representative spike (spike 3) detected by SEEG (upper panel each contact refers to the right mastoid electrode) and MEG (middle panel), and MEG spike dipole superimposed on the patient's cortical surface (lower panel). In this study, the spatial relationship between MEG dipole and SEEG contact location was investigated. Amplitude was calculated from the peak to trough measurement.

Results

Figure 2 shows the raw waveforms of a representative spike (spike 3) using SEEG and MEG, and the estimated dipole on the patient's brain image. *Figure 3A* shows the spatial relationship between C' electrode and all eight MEG spike dipoles. *Figure 3B* shows the coronal and axial slice of brain images constructed from the MRI. Each cylinder in *figure 3A and 3B* represents a contact with the C' electrode. Dots indicate the MEG dipole locations of all eight spikes. From these images, distance between each MEG spike dipole and each SEEG contact was calculated. As shown in *figure 4*, for all spikes, we were able to use a quadratic fall-off curve

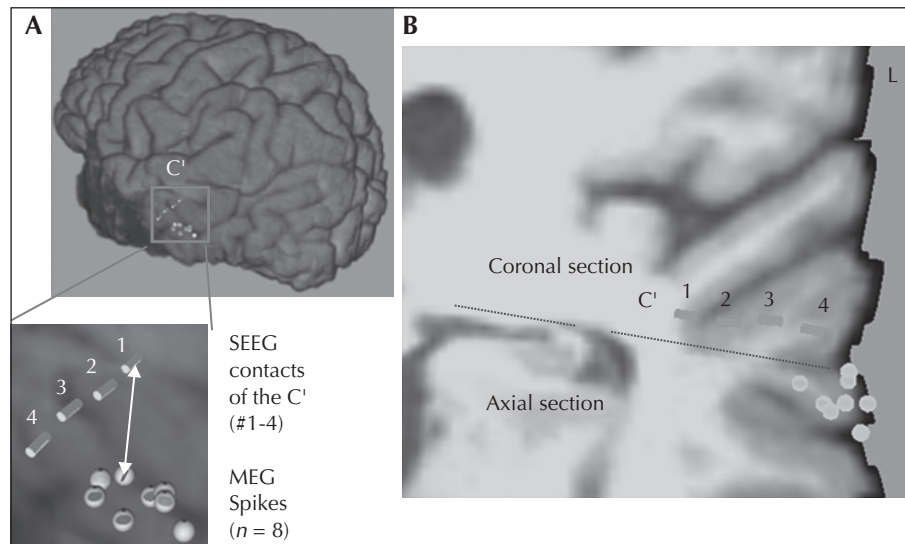


Figure 3. (A) Brain surface image highlighting the involved C' electrode and the associated MEG spike dipoles. (B) Three dimensional view of coronal and axial cut of brain images constructed from three dimensional MRI Dots indicate all eight spike dipoles selected in the study Three dimensional distance between each spike dipole and each SEEG contact is calculated (one example is shown by the white arrows) Cylinders indicate C' SEEG contacts; C'1 is the most mesial contact and C'4 the most lateral.

to approximate the relationship between the amplitude (y axis) and the distance from the modelled MEG dipole to each SEEG contact (x axis) ($R^2 > 0.80$).

Discussion

The quadratic fall-off approximation, with a high R^2 value between electrical amplitude (μV) recorded in the SEEG contact, and distance from the MEG dipole to each SEEG contact is consistent with volume conduction, *i.e.* potential is inversely proportional to increase of distance (Patton and Woodbury, 1965). This result supports the concept that the MEG dipoles reflect the “centre” of spike location, or at least a subset of spikes captured at the recording. MEG may provide comprehensive information for SEEG, which records spike activities directly but is inherently limited in spatial sampling. Unlike MEG, in which magnetic signals would be less distorted with resistive properties of skull and scalp, this is especially problematic for EEG after previous craniotomy. Therefore, it would be advantageous to use MEG for spike source localisation in cases such as ours (Barkley and Baumgartner, 2003; Tang *et al.*, 2003). In fact, the improved accuracy of localisation of MEG, compared to scalp EEG for epileptiform discharges, has been proven by evaluating the concordance with intracranial recording and/or postsurgical outcome to the sublobar level reported by Knowlton *et al.* (2006). The source locations determined by MEG are presumed to be in the epileptogenic zone, but the precise boundaries of the epileptogenic

zone are unclear (Barkley and Baumgartner, 2003) and SEEG lead field characteristics are currently unknown. Compared to subdural electrodes, SEEG can more effectively record deeper sources, although there are also patients in whom the epileptogenic focus may not be detected by SEEG, resulting in postoperative poor seizure outcome (Spencer, 1981).

Although the distance-amplitude relationship was not always straightforward (the nearest contact does not always show the highest amplitude, as shown for spike 5), it is still notable that a high R^2 value (over 0.80) of quadratic fall-off curve was successfully achieved for all spikes, suggesting that the variability of electrical magnitude recorded in each contact does not affect the overall conclusion.

This study only addresses the relationship between dipole location and maximal electrical field potential for those spikes which can be seen by MEG. In our patient, the basal temporal spikes were not detected, as sources from deep mesial structures are often unresolved by MEG which may be less sensitive to such structures. This was demonstrated by Oishi *et al.* in their 2002 study, in which they applied simultaneous electrocorticography (ECoG) and MEG in two patients with lateral frontal epilepsy or basal temporal lobe epilepsy. They reported that in the lateral frontal case, 53% of ECoG spikes were detected by MEG, the majority of which activated three subdural electrodes. In their basal temporal case, only 26% ECoG spikes were detected by MEG, but none that activated only three subdural electrodes (Oishi *et al.*, 2002). They speculated that the reason why the MEG sensor was less

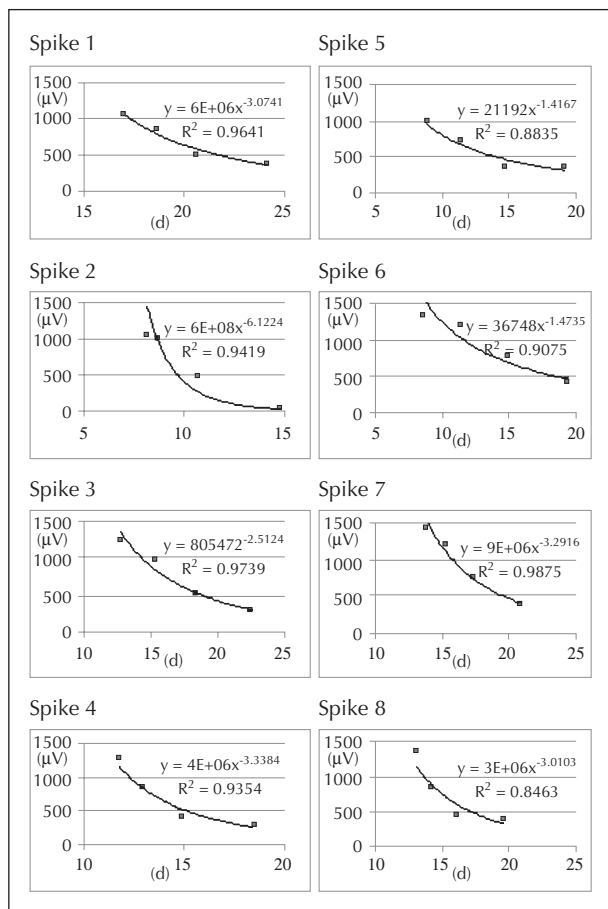


Figure 4. Relationship between electrical amplitude (μV ; >y axis) recorded in each SEEG contact and distance (d mm; >x axis) from each MEG spike dipole to the SEEG contacts are shown for all eight spikes. Note that approximation with quadratic fall-off with a high R^2 value (greater than 0.80) is accomplished in all spikes.

sensitive for the basal temporal source was because of depth. This speculation is consistent with our case, in which MEG was also blind to basal temporal source. As the “gold standard” for invasive recording, the ability to detect spikes from deep sources such as medial temporal structures by MEG, as well as EEG, has long been debated. By comparing interictal ECoG and MEG findings, Agirre-Arrizubieta *et al.* showed that less than 25% of all spikes from the mesial temporal region were detectable using MEG (Agirre-Arrizubieta *et al.*, 2009). By performing simultaneous SEEG and MEG in three mesial temporal epilepsy patients, Santiuste *et al.* showed that about 25 to 60% of spikes were detected using MEG (Santiuste *et al.*, 2008). Interestingly, Wennberg *et al.* reported that for spikes from mesial temporal structures, current noninvasive EEG and MEG source localisation studies do not accurately identify their true source, based on the findings that spikes recorded using EEG and MEG in mesial temporal lobe epilepsy were localised to neocorti-

cal foci and not to the mesial temporal structures (Wennberg *et al.*, 2011). Based on these reports, careful patient screening is needed for MEG and simultaneous SEEG-MEG recording. Further studies are needed to clarify the appropriate group of patients for both modalities.

In conclusion, this study suggests that simultaneously recorded SEEG and MEG provide complementary additional and more precise spatial localisation information. The role of MEG for epilepsy patients undergoing invasive monitoring is not only to guide the placement of SEEG or subdural grids preoperatively, but also to clarify the location of sources during the post-implantation monitoring phase. □

Disclosures.

This work was supported, in part, by the National Institutes of Health under grants R01-EB009048 and R01-NS074980, and by the Epilepsy Center of the Cleveland Clinic Neurological Institute. None of the authors has any conflict of interest to disclose.

References

- Agirre-Arrizubieta Z, Huiskamp GJ, Ferrier CH, van Huffelen AC, Leijten FS. Interictal magnetoencephalography and the irritative zone in the electrocorticogram. *Brain* 2009; 132: 3060-71.
- Barkley GL, Baumgartner C. MEG and EEG in epilepsy. *J Clin Neurophysiol* 2003; 20: 163-78.
- Hari R, Lounasmaa OV. Recording and interpretation of cerebral magnetic fields. *Science* 1989; 244: 432-6.
- Knowlton RC, Laxer KD, Aminoff MJ, Roberts TP, Wong ST, Rowley HA. Magnetoencephalography in partial epilepsy: clinical yield and localization accuracy. *Ann Neurol* 1997; 42: 622-31.
- Knowlton RC, Elgavish R, Howell J. Magnetic source imaging versus intracranial electroencephalogram in epilepsy surgery: a prospective study. *Ann Neurol* 2006; 59: 835-42.
- Matsumoto R, Nair DR, LaPresto E, *et al.* Functional connectivity in the human language system: a cortico-cortical evoked potential study. *Brain* 2004; 127: 2316-30.
- Medvedovsky M, Taulu S, Bikmullina R, Paetau R. Artifact and head movement compensation in MEG. *Neurol Neurophysiol Neurosci* 2007; 29: 4.
- Oishi M, Otsubo H, Kameyama S, *et al.* Epileptic spikes: magnetoencephalography versus simultaneous electrocorticography. *Epilepsia* 2002; 43: 1390-5.
- Patton HD, Woodbury JW. Special properties of nerve trunks and tracts: potentials in a volume conductor. In: Ruth TC, Patton HD, Woodbury JW, Towe AL, eds. *Neurophysiology*. Philadelphia: Saunders, 1965: 73-94.
- Santiuste M, Nowak R, Russi A, *et al.* Simultaneous magnetoencephalography and intracranial EEG registration: technical and clinical aspects. *J Clin Neurophysiol* 2008; 25: 331-9.

Song T, Cui L, Gaa K, *et al.* Signal space separation algorithm and its application on suppressing artifacts caused by vagus nerve stimulation for magnetoencephalography recordings. *J Clin Neurophysiol* 2009; 26: 392-400.

Spencer SS. Depth electroencephalography in selection of refractory epilepsy for surgery. *Ann Neurol* 1981;9: 207-14.

Talairach J, Bancaud J, Bonis A, Szikla G, Tournoux P. Functional stereotaxic exploration of epilepsy. *Confin Neurol* 1962; 22: 328-31.

Tang L, Mantle M, Ferrari P, *et al.* Consistency of interictal and ictal onset localization using magnetoencephalography in patients with partial epilepsy. *J Neurosurg* 2003; 98: 837-45.

Wang ZI, Jin K, Kakisaka Y, *et al.* Imag(in)ing seizure propagation: MEG-guided interpretation of epileptic activity from a deep source. *Hum Brain Mapp* 2012, in press. doi: 10.1002/hbm.21401

Wennberg R, Valiante T, Cheyne D. EEG and MEG in mesial temporal lobe epilepsy: where do the spikes really come from? *Clin Neurophysiol* 2011; 122: 1295-313.